Bulletin of the Seismological Society of America, Vol. 93, No. 3, pp. 986–997, June 2003

# Lithology and Shear-Wave Velocity in Memphis, Tennessee

by J. Gomberg, B. Waldron, E. Schweig, H. Hwang, A. Webbers, R. VanArsdale, K. Tucker, R. Williams, R. Street, P. Mayne, W. Stephenson, J. Odum, C. Cramer, R. Updike, S. Hutson, and M. Bradley

Abstract We have derived a new three-dimensional model of the lithologic structure beneath the city of Memphis, Tennessee, and examined its correlation with measured shear-wave velocity profiles. The correlation is sufficiently high that the better-constrained lithologic model may be used as a proxy for shear-wave velocities, which are required to calculate site-amplification for new seismic hazard maps for Memphis. The lithologic model and its uncertainties are derived from over 1200 newly compiled well and boring logs, some sampling to 500 m depth, and a moving-least-squares algorithm. Seventy-six new shear-wave velocity profiles have been measured and used for this study, most sampling to 30 m depth or less. All log and velocity observations are publicly available via new web sites.

## Introduction

The U.S. Geological Survey (USGS) is producing seismic hazard maps at a 1:24,000 scale for three major U.S. metropolitan areas, one of which is Memphis, Tennessee (Fig. 1). We employ the same methodology and inputs to generate the Memphis maps as used in the updated USGS national seismic hazard maps for the central and eastern United States (Frankel *et al.*, 1996, 1997). Unlike the national maps, however, the Memphis maps will include the amplification and nonlinear effects of local shallow geologic structure on ground motions. This inclusion necessitates developing a model of the geologic structure, characterized in terms of shear-wave velocity, which is the material property that most strongly influences the ground motions (see Field *et al.* [2000] for a recent summary of ground-motion site effects).

The primary objective of this study was to determine if lithologic structure, which is more densely sampled, might be used to interpolate between sparsely sampled shear-wave velocity profiles. Numerous studies elsewhere show correlation between lithology and shear-wave velocity profiles (e.g., Field *et al.*, 2000; Wills *et al.*, 2000). Results of this study, combined with new geologic maps, permit shear-wave velocity profiles to be estimated throughout Memphis. These profiles provide needed input to site-response calculations for new seismic hazard maps of the city.

Approximately 90 new shear-wave velocity profiles were collected in and around the Memphis area as part of the Memphis, Shelby County, hazard mapping project (as noted below, not all 90 were used in this analysis). Although this is a significant improvement over what existed prior to beginning this effort, characterization of the structure in terms of velocity still requires extrapolation between measured sites. We have attempted to extrapolate between measured velocity profiles in a geologically meaningful way. We hypothesized that the shear-wave velocities depend strongly on the lithology and, thus, mapped the lithology using geophysical well logs and soil boring logs that sample the region much more densely than do the velocity profiles (Fig. 1). At the sites of all velocity profiles we attempted to correlate profile layer depths with lithologic layer interface depths estimated from the logs and then assigned velocities to corresponding lithologic layers. There were a sufficient number of profiles to do this for five lithologic units, reaching depths of approximately 30 m. The spread of shear-wave velocities for a given lithologic layer indicates that lithology can be used as a proxy for shear velocity, such that velocity ranges can be associated with each of the five lithologic units, although the ranges overlap somewhat.

One product of this work is a three-dimensional model of the shallow lithology beneath Memphis. In this article we describe our approach to deriving this lithologic model, the resulting model and its uncertainties, and an analysis of the relationship between lithologic units and shear-wave velocity. The lithologic model is constrained by more than 1200 logs sampling to 10–15 m depth, and a sufficient number exist to derive the general shape of layer interfaces as deep as about 500 m. Although not our primary objective, we expect that the lithologic model alone may be of interest to those studying the local geology, tectonics, and hydrology.

## Lithologic Model

### Geologic Summary

Memphis and Shelby County are situated in the north-central portion of the Mississippi embayment, a sediment-

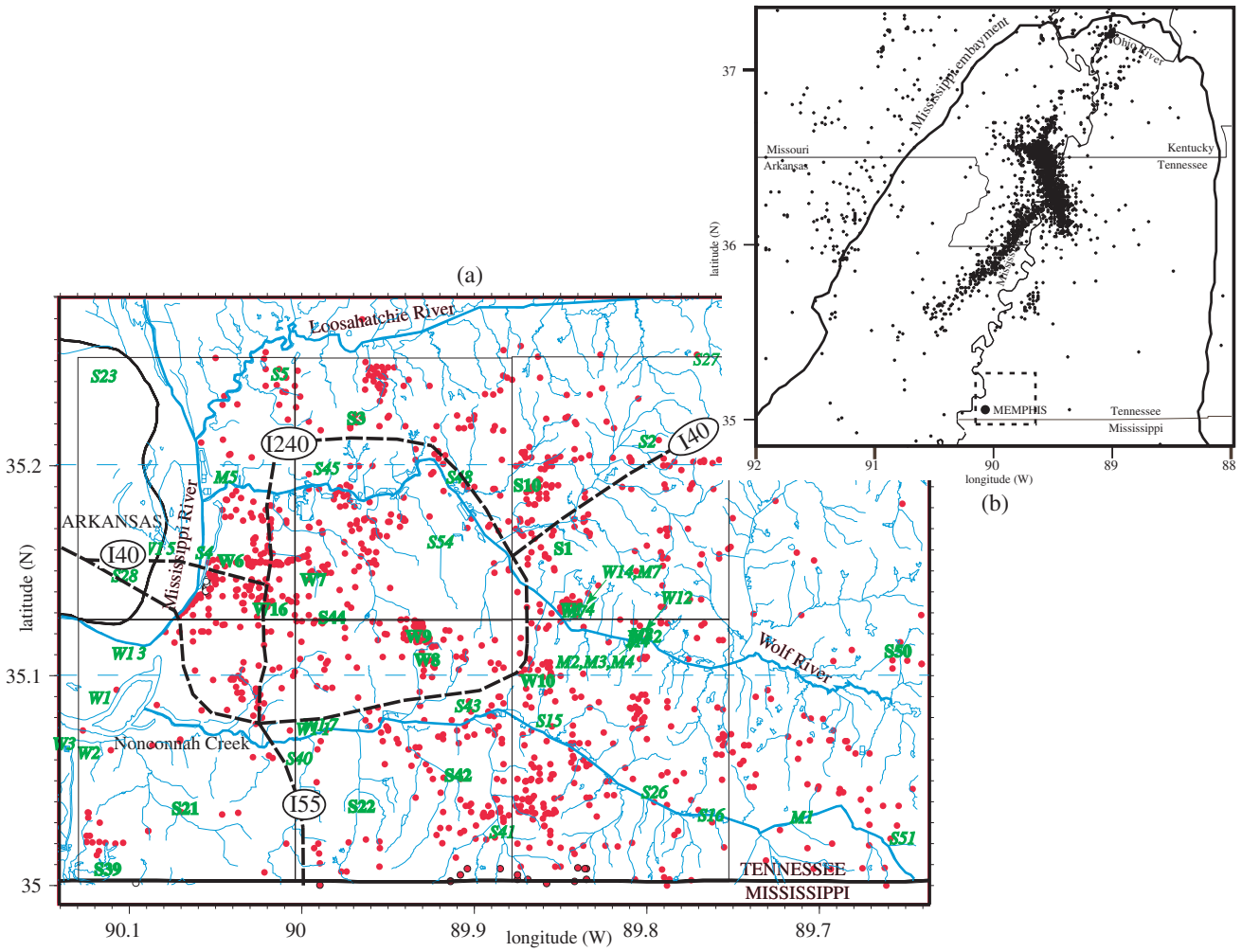


Figure 1. (a) Map of Memphis and vicinity showing the locations where geophysical well log and soil boring logs (red circles) and shear-wave velocity profiles (green letter/number labels) were measured. (Different letters refer to the group that made the measurement, and numbers are arbitrary.) Major waterways (dark blue lines) are labeled and tributaries shown, as well as interstate highways (thick dashed black lines). Shear-wave velocity profiles identified as having an alluvial surficial layer are italicized. Results of this study will be used to produce seismic hazard maps for the six 7.5′ quadrangles outlined. (b) The location of the study area (dashed box) within the Mississippi embayment. The epicenters of earthquakes cataloged since 1974 are shown by pluses.

filled northeast–southwest–trending syncline that formed as a result of Cretaceous tectonics and Cretaceous and Tertiary sediment loading (Fig. 1) (Cox and VanArsdale, 2002; VanArsdale and TenBrink, 2000). The embayment plunges southward along an axis roughly aligned with the Mississippi River and overlies the New Madrid seismic zone. The seismic zone hosted the three largest earthquakes in the continental United States during historical times and currently is the most seismically active region east of the Rocky Mountains (Johnston and Schweig, 1996). The faulting that resulted from these earthquakes is obscured by thick sequences of unconsolidated (i.e., unlithified) embayment sediments. No regionally extensive consolidated rock units exist above the Paleozoic bedrock, which is ~900 m below land surface (Graham and Parks, 1986). We summarize the stratigraphy of these sediments below (see also Table 1).

The city of Memphis is built on a flat upland of windblown loess (a fine sandy silt) deposited during glacial periods until approximately 10,000 years ago. When eroded, the loess can form vertical walls up to 24 m high. At the base of the loess are Plio-Pleistocene Lafayette Formation (Upland Gravel) sand and gravel deposits that vary from 0 to 33 m thick. Beneath these sands and gravels lie hundreds of meters of interbedded lenticular sands, silts, and clays deposited in marine and nonmarine shallow-water environments during the Tertiary and Late Cretaceous. The Tertiary section can reach up to 460 m thick beneath the Memphis area and includes sediments from the Paleocene, Eocene,

Table 1
Lithologic Units

| Unit/Group (Age) | Description | ~Depth to Unit Top (m) | Mean ± Std (Median, Weighted Mean) Shear-Wave Velocity (m/sec) |
|---|---|---|---|
| Floodplain sediments and man-made fill (Holocene and Pleistocene) | Alluvial, unconsolidated, poorly to moderately well stratified silt, sand, and gravel | 0 | 171 ± 24 (174, 172) |
| Loess (Pleistocene) | Eolian, unconsolidated, poorly stratified glacial silts and fine sands | 0 | 192 ± 37 (195, 192) |
| Lafayette Formation (Pleistocene and Pliocene) | Weakly to strongly indurated clay, silt, sand, gravel, and cobbles, locally iron oxide cemented | 3–15 | 268 ± 72 (265, 268) |
| Jackson, Cockfield, and Cook Mountain/ Upper Claiborne (Eocene) | Dense clays, silts, and fine sands with organic fragments | 6–30 | 413 ± 105 (408, 421) |
| Memphis Sand/Lower Claiborne (Eocene) | Fine to coarse sands interbedded with thin layers of silt and clay | 20–80 | 530 ± 134 (553, 515) |
| Flour Island/Upper Wilcox (Paleocene) | Dense clays, with fine-grained sands and lignite | 200–350 | |
| Fort Pillow Sand/Middle Wilcox (Paleocene) | Well-sorted sands with minor silt, clay, and lignite horizons | 300–400 | |
| Old Breastworks/Lower Wilcox (Paleocene) | Dense clays and silts, with some sands and organic layers | 300–500 | |

The weights used to calculate the weighted mean velocities (values on right in parentheses) are either 1.0 when the velocity profile layer interfaces are within the estimated lithologic boundary depth estimates or 0.5 when they are not. The Lafayette Formation is not designated as such in Tennessee by the hydrologic community, but rather is referred to as Fluvial or Terrace Deposits. We use the name most familiar to the geologic and geophysical community.

and some Plio-Pleistocene series. The Eocene-aged Claiborne Group is divided into an upper unit and a lower unit, which is of particular interest to hydrologists for its water-bearing properties. The upper Claiborne unit ranges from 0 to 110 m thick and consists of, in descending order, the (sometimes present) Jackson Formation (a mostly sand and clay unit), the Cockfield Formation (distinguished by its abundance of clay), and the Cook Mountain Formation (mostly sand with some clay). The lower Claiborne unit is comprised of the Memphis Sand, a 180- to 275-m thick fine to very coarse sand with discontinuous clay lenses and discontinuous lignite deposits. The Memphis Sand is a major aquifer, providing over 190 million gallons of water per day to the city (Parks and Carmichael, 1990; Kingsbury and Parks, 1993).

Beneath the Memphis Sand is a 49- to 95-m thick Paleocene series clay-confining layer, known as the Flour Island, which separates the Memphis Sand from the underlying Fort Pillow Sand, another important water-bearing formation for the city of Memphis. Beneath the Tertiary system lie about 200 m of Cretaceous-aged sediments that rest unconformably on the Paleozoic bedrock and dip generally toward the west. Differential erosion and localized deposition of the unconsolidated layers has resulted in abrupt facies changes, which can make distinctions of specific formations difficult.

### Geophysical Well Logs and Soil Boring Logs

More than 1200 geophysical well logs and soil boring logs from in and around the Memphis area were compiled from a variety of sources and the depths to the interfaces between major lithologic units identified. The well logs sample the interfaces, the deepest to slightly below ~500 m. These logs were measured for groundwater exploration and monitoring purposes and record geophysical properties of the sediments, primarily spontaneous potential, resistivity, and gamma-ray emission. Most of these logs were taken from the Ground Water Site Inventory database, maintained by the USGS's water resources division. Parks and Carmichael (1990) and Kingsbury and Parks (1993) used several hundred of these logs and geologic information to infer the existence of several faults thought to displace the unconsolidated Tertiary sands (Memphis Sand and Fort Pillow) beneath Shelby County. The soil boring logs are much more numerous but sample only the top 10–15 m or less and include geotechnical measurements (e.g., standard penetration tests) and properties of the sediments (e.g., grain size, stiffness, moisture content, etc.).

All relevant information about the logs is available in a Geographic Information System (GIS) database accessible by the public through a web or ArcView interface; see http://gwidc.gwi.memphis.edu/website/introduction for informa-

tion about this database and how to access it. Table 1 lists the eight units identified, in order of their depth in the stratigraphic column. The thickness of the unconsolidated sedimentary column beneath Memphis extends several hundred meters beneath the maximum depth sampled by the logs. Although the deeper structure is important from the perspective of estimating site amplification, particularly at periods of several seconds or more, it must be constrained by other means from other studies (e.g., Dart and Swolfs, 1998; Bodin and Horton, 1999; VanArsdale and TenBrink, 2000).

## Modeling Lithologic Boundaries

Our first objective is to estimate the depths of a lithologic boundary at any location, using irregularly distributed geophysical well and soil boring log data as constraints. We do not require these constraints to be satisfied exactly, but rather we fit surfaces instead of interpolating between measurements of boundary depths. We attempt to estimate the boundary depths in such a way that we can quantify some of the uncertainty in our depth estimates. Uncertainties exist because of unaccounted for random and deterministic processes that may be natural or result from instrumental or procedural error. Because the processes that determine the stratigraphy (deposition, erosion, faulting, etc.) are too complex to be described by some physical mathematical model, we describe them empirically (i.e., using polynomials that have no physical meaning). This empirical description may not be well constrained everywhere by the observations, which leads to "modeling" or extrapolation error. We assume, however, that it is sufficient to predict the characteristics of the data reflecting the deterministic processes. The difference between these predicted and observed data thus provides an estimate of the random or "data" error. These data errors may reflect the subjectivity required to identify a logged signal as a lithologic change (particularly if the boundary is gradational), instrumental and human error, and real variability on scales smaller than that we are concerned with. In the following sections we describe our approach to estimating the boundary depths and their uncertainties.

We employ a moving-least-squares algorithm (Lancaster and Salkauskas, 1986) to derive a model of the depth of each lithologic boundary, $d_{\mathrm{mod}}(x,y)$. At each location, $x,y$, the boundary is represented by a polynomial with location-dependent coefficients, $b_i(x,y)$, $i = 1,6$. We find this allows the variability expected to result from geologic and hydrologic processes to be modeled. Higher-order polynomials could be used but may result in modeling observational noise and in modeling variability at scales unimportant for seismic hazard calculations. The modeled depth is

$$d_{\mathrm{mod}}(x,y) = b_1(x,y) + b_2(x,y)\,x + b_3(x,y)\,y + b_4(x,y)\,x^2 + b_5(x,y)\,y^2 + b_6(x,y)\,xy. \quad (1)$$

Details of this moving-least-squares algorithm and our approach to estimating modeling and data errors, $\sigma(x,y)_{\mathrm{mod}}$ and $\sigma(x,y)_{\mathrm{dat}}$, respectively, are described in the Appendix.

Map and cross-sectional views of the stratigraphy estimated from the geophysical well log and soil boring log observations are shown in Figures 2 and 3, respectively. Map views (Fig. 2) show the depths to the top of each lithologic unit (Table 1). Quantitative estimates of $\sigma(x,y)_{\mathrm{mod}}$ and $\sigma(x,y)_{\mathrm{dat}}$ are shown on the two east–west cross sections plotted in Figure 3. In some areas, estimated depths are nearly unconstrained by measurements from within the area. Rather than not show any estimated boundary depths in these areas, we show both the locations of the logs as guides to the uncertainties in Figure 2 and quantitative uncertainties in Figure 3. Eliminating some regions from our mapped boundary estimates would require setting some threshold of required number of measurements, which we do not know how to do in a meaningful way. Moreover, if we imposed some minimum measurement threshold requirement consistently, information about the deeper layers would be lost. Indeed some nearly unconstrained shallow boundary estimates may be erroneous, but deeper layers constrained by very few measurements probably still have meaningful features (i.e., slope trends). We hypothesize that this is because the deeper layers probably naturally vary less abruptly and the magnitudes of the depth changes across the region are much greater than for the shallow units.

Several general characteristics are resolved in these modeled lithologic boundaries. All boundaries deepen from east to west, with a southeast–northwest deepening resolvable in the boundaries starting at the top of the Lafayette Formation sands and gravels to the top of the Memphis Sand. The combined Jackson, Cockfield, and Cook Mountain Formations thicken westward from about 20 m to as much as 60 m. These units cap the Memphis Sand, which is found as shallow as about 25 m depth in the east to ~80 m depth in the west (in the region where it is well resolved). This unit also thickens by ~80 m westward, to a thickness of several hundred meters. Below the Memphis Sand the scarcity of observations only permits resolution of a general downward dip of the Flour Island and Fort Pillow Sand toward the west.

We comment briefly on the estimated uncertainties, $\sigma(x,y)_{\mathrm{mod}}$ and $\sigma(x,y)_{\mathrm{dat}}$, to demonstrate that they appropriately represent the random and modeling uncertainties as described above. This is important if one intends to interpret any of the mapped features in terms of geologic, tectonic, or hydrologic processes, requiring knowledge of what features are really resolved. Previous studies employing log data from broader areas within and including the Mississippi embayment include studies of the local hydrology (Kingsbury and Parks, 1993), the regional tectonics (Mihills and VanArsdale, 1999; VanArsdale and TenBrink, 2000), and the regional geology (Fisk, 1939; Dart and Swolfs, 1998). Additionally, the log data we use augment other observations used to construct geologic cross sections that will accompany new 1:24,000-scale geologic maps of Memphis (Broughton *et al.*, 2001). The magnitude of $\sigma(x,y)_{\mathrm{dat}}$ is comparable to the difference between observations over the distance from $x,y$ within which the observations are equally

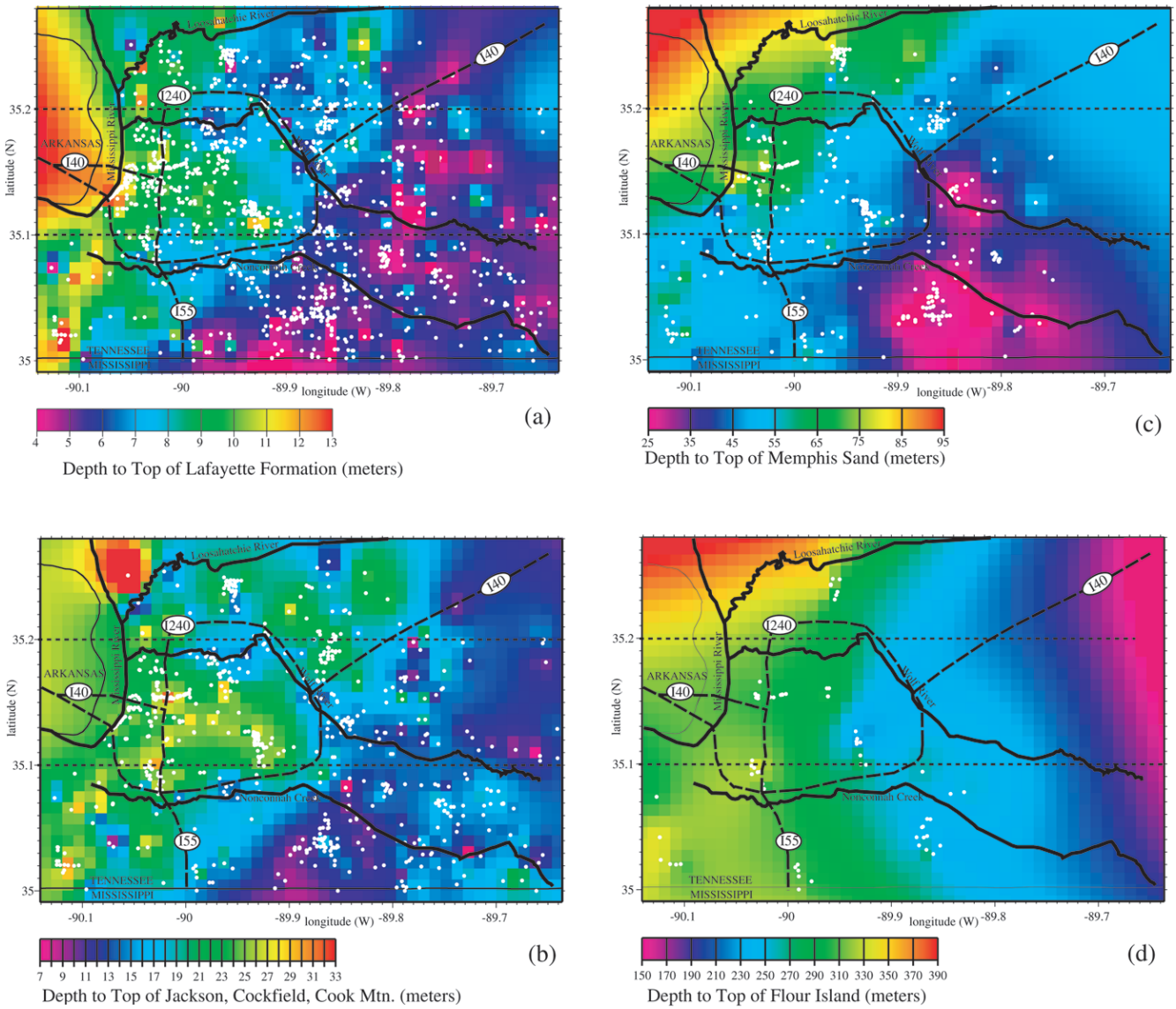


Figure 2. Depths to the top of the lithologic layers listed in Table 1, estimated using the procedure described in the text on a 1-km spaced grid. Depths are referenced from the National Elevation Datum. White dots indicate locations of geophysical well log and soil boring log observations that constrain each surface; where there are no observations the depths are nearly unconstrained. East–west dashed lines show locations of cross sections in Figure 3. Cross sections also show quantitative uncertainty estimates. (a) Lafayette Formation sands and gravels. Geologic mapping shows the Lafayette Formation has been scoured away by the river west of the Mississippi River bluff line. Thus, the depths shown in this area are unconstrained. (b) Upper Clairborne Group Jackson, Cockfield, and Cook Mountain Formations. (c) Memphis Sand. (d) Flour Island. (e) Fort Pillow. (f) Old Breastworks.

weighted, chosen to be 100 m ($\varepsilon$ in equation A3), and thus, they seem to appropriately represent the random variability between measurements. These data uncertainties exceed $\sigma(x,y)_{\text{mod}}$ everywhere except toward the edges of the region where the observations become sparse in number; that is, the greatest uncertainty exists where the model is purely an extrapolation from distant data. This can be seen by comparing the distribution of observation points in Figure 2 with the uncertainties shown on the cross sections in Figure 3. Generally, $\sigma(x,y)_{\text{mod}}$ decreases inversely with the number of observations in the vicinity of $x,y$, until it settles at some very small value. This occurs when the polynomial fit becomes insensitive to the omission or addition of a few data. For some units in regions where there are no data, $\sigma(x,y)_{\text{mod}}$ does not adequately represent the uncertainty (e.g., west of the Mississippi River bluff line in Arkansas; Figs. 2 and 3). This

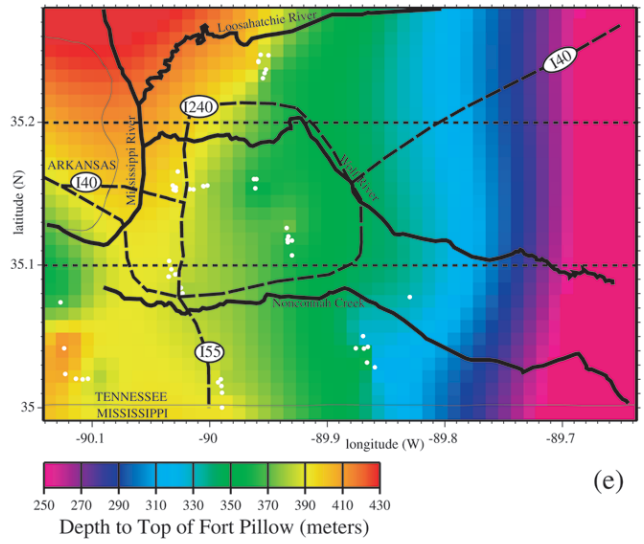


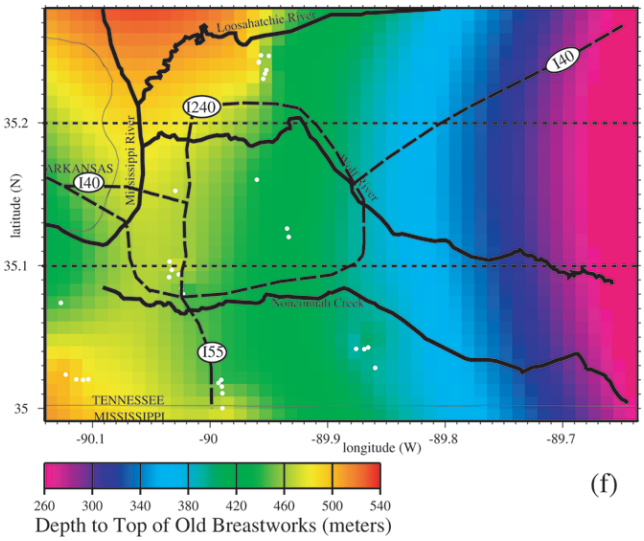


is generally not problematic, however, as the areas where there are few or no data usually lie outside the region of interest. In summary, the characteristics of $\sigma(x,y)_{\mathrm{dat}}$ and $\sigma(x,y)_{\mathrm{mod}}$ seem to sensibly capture and quantify the random and deterministic uncertainties in the estimates.

## Correlation of Velocity with Lithology

At the location of each of 76 shear-wave velocity profiles used in our analysis (Fig. 1) we estimated the depth to each lithologic unit using the procedure described above. Although 90 profiles were measured, those outside our study area or that sampled only the top few meters were not used. We then assigned velocities to each lithologic unit, thereby obtaining up to 76 estimates of velocity for each unit. If lithology provides a useful proxy for velocity, these velocity estimates should cluster tightly around a single value for each unit. We did not use the layer interface depths estimated from the velocity profiles as constraints on the lithologic model because part of our objective was to determine how well the lithology inferred from the logs alone correlated with the velocity.

The velocity profiles were measured using refraction, a combination of refraction and reflection, and a seismic piezocone that measures interval velocities (see Schneider *et al.*, 2001, Street *et al.*, 2001 and Williams *et al.*, 2003 for more details). Romero and Rix (2001) provided discussion of a detailed analysis of the variability among profiles measured within tens of meters of one another, arising from the use of different measurement techniques and real structural heterogeneity. With the exception of the piezocone measurements, which provide interval velocity estimates, velocity profiles are represented as a series of plane layers with average velocities assigned to each layer. Because log observations correspond to the top of the units and the fit surfaces are continuous while the real surficial units (the loess and alluvium) are not, we identify the top layer as either alluvium or loess using new geologic maps of Memphis. For our purposes, we classified all sites simply as alluvium regardless of whether the surface materials were mapped as artificial fill, alluvium, river terrace, sand, or silt (see locations on Fig. 1). A few sites located on roadway fill but distant from any major waterway were designated as loess, because the fill thickness was likely to be insignificant.

Approximately 70% of the velocity layer interface depths agreed with the inferred lithologic boundary depths within the uncertainties estimated for the latter (Fig. 4). This suggests that lithology is a useful indicator of shear velocity, but also that other factors affect the shear velocity. For example, Bodin *et al.* (2001) noted in their study of resonant microtremor observations in the Mississippi embayment that the average shear wave velocity appears to correlate better with sediment thickness than geological layering within the sediments. In the remaining 30% of the velocity profiles for which velocity layer interfaces did not correspond to estimated lithologic boundary depths, lithologic units were simply assigned to velocity profile layers based on their stratigraphic order. Several profiles contained thin high-velocity layers, thought to be lenses of cemented sediments within the Lafayette Formation sands and gravels, which we neglected when estimating the unit velocity. A few profiles also contained very thin (<2-m thick) high-velocity layers at the surface, which we also neglected. Figure 5 shows histograms of the velocities for each lithologic unit. Mean and median values are also listed in Table 1.

Romero and Rix (2001) and Williams *et al.* (2003) analyzed the same shear-wave velocity profiles we used, along with others from the surrounding area. Both studies looked at the individual profiles in more detail and attempted to correlate shear-wave velocities with sediment age and type, which they estimated from published geologic information. They also distinguish Mississippi River alluvium from that

Figure 2. (*Continued*)

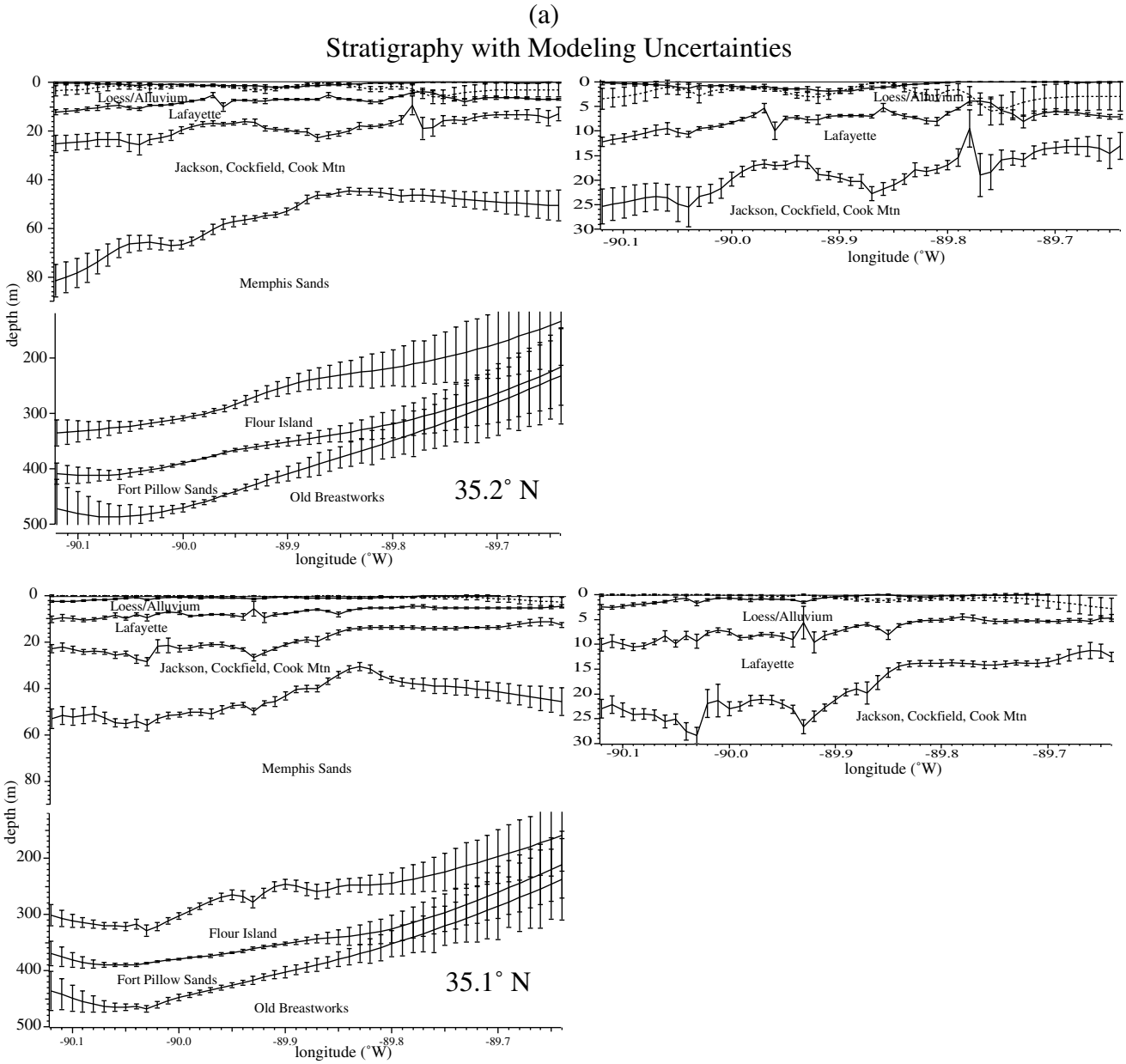


along other waterways, which we do not do. Romero and Rix (2001) found all surficial alluvial deposits have shear-wave velocities of 158–200 m/sec (we estimate ~170 m/sec) and thicknesses of 9–14 m except along the Mississippi River, where they are thicker. Williams *et al.* (2003) averaged profiles sampling only Mississippi River alluvium, including some that we did not, and found an average shear-wave velocity of 206 m/sec. Although this slightly higher estimate is within the spread of our measurements (Fig. 5), it corresponds to a National Earthquake Hazard Reduction Program (NEHRP) classification of site category D, rather than the category E implied by our lower estimate (NEHRP, 1997). This highlights the need to do site-specific analyses when such distinctions are considered important. Romero and Rix (2001) estimated loess velocities of 176–274 m/sec and a thinning eastward from a maximum along the bluffs of 14 to 6 m thick in the southeast of the study area (Fig. 1). We do not estimate the alluvium and loess thicknesses as precisely, but our loess thicknesses of 3–15 m agree well with theirs. Our loess velocity estimates of ~190 m/sec are well within Romero and Rix's estimated range and agree well with the Williams *et al.* (2003) estimate of an average of 210 m/sec.

Lafayette Formation shear-wave velocities estimated by Romero and Rix (2001) are in the range 280–560 m/sec and extend to depths of 28 m. The underlying Jackson and Upper Claiborne units have slightly higher shear-wave velocities and extend to 40 m depth. Williams *et al.* (2003) found a combined Lafayette/Upper Claiborne unit average velocity of 455 m/sec. We estimate values for the Lafayette Forma-

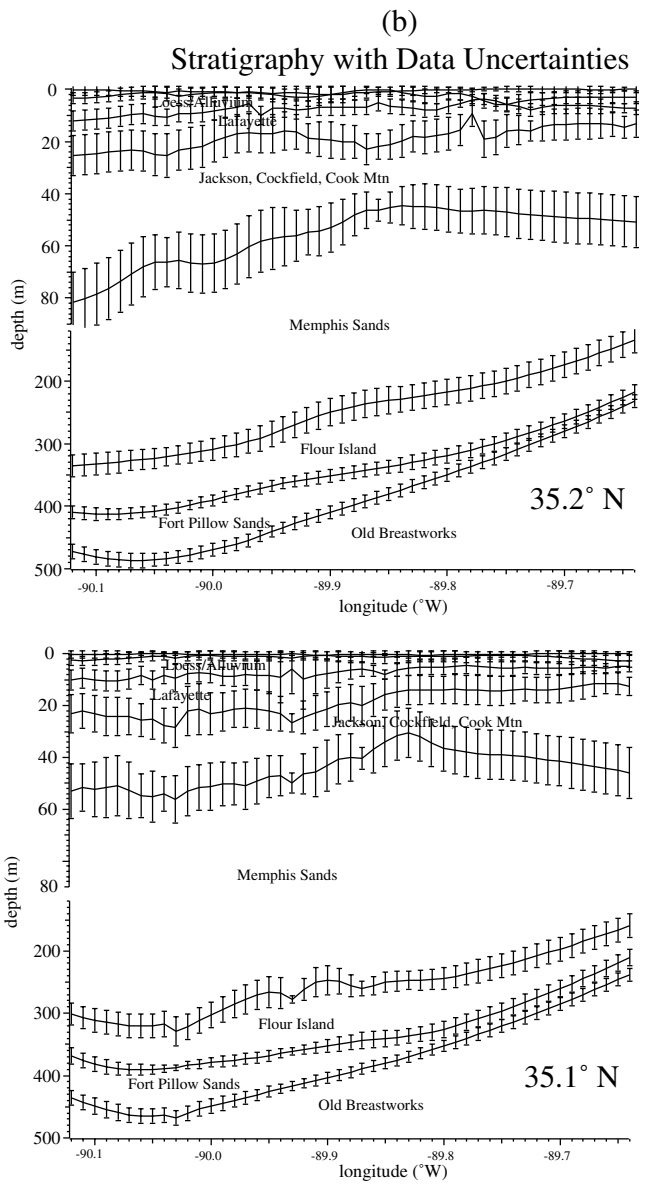


Figure 3. Cross sections of estimated depths to lithologic boundaries at 35.1°N and 35.2°N (dashed lines in Fig. 2). Note the change of vertical scale at 90 m. (a) Depths and modeling uncertainties, $\sigma_{mod}$ for the entire section sampled (left) and an expanded view of the shallower layers (right). (b) Depths and data uncertainties $\sigma_{dat}$. The estimation algorithm essentially finds an average depth at a specified location $x,y$ from measurements within ~100 m (see text). Note that the uncertainty in a measured depth to some lithologic boundary from a single log may be considerably less than the variability in depths over small distances, resulting from erosional, depositional, and perhaps tectonic processes; $\sigma_{dat}$ represents this variability and is comparable to the difference between observations separated by ≤100 m.

tion of ~265 m/sec and for the layers beneath 410 m/sec, respectively. When the uncertainty in these is considered, the three studies' results are consistent. Our slightly lower mean or median estimates may in part reflect the fact that we have omitted thin high-velocity layers and they have not. Although the data sampling the Memphis Sand shear-wave velocities are sparse, shear-wave velocity estimates for this unit of 536–569 m/sec (Romero and Rix, 2000) and an average of 534 m/sec (Williams *et al.*, 2003) are consistent with ours of ~530 m/sec. Only a single shear-wave velocity profile extending below the Memphis Sand has been measured, and that was after this study was completed. A few deeper compressional-wave velocity profiles exist, only one of which is from Memphis at the same site where the shear-wave velocity profile was measured. Thus, little data exists on which to base inferences about the characteristics of the shear-wave velocities beneath the Memphis Sand.

## Discussion and Conclusions

Numerous studies similar to ours have been completed in California, although to our knowledge none have been done within the Mississippi embayment. We compare our results to those of two of the most recent studies for California. Both use much larger datasets and only surficial geologic maps, rather than looking at stratigraphic units in profile. Wills *et al.* (2000) used 1:250,000-scale maps for all of California and grouped various geologic units according to characteristics expected to have similar shear-wave velocities, and they compared these to the average shear-wave velocity in the upper 30 m, or $V_s30$. The degree of correlation between surficial geology and $V_s30$, as measured by the spread of histograms like those in our Figure 5, is very comparable to our results. Wills *et al.* (2000) concluded that geologic units provide useful proxies for estimating shear-

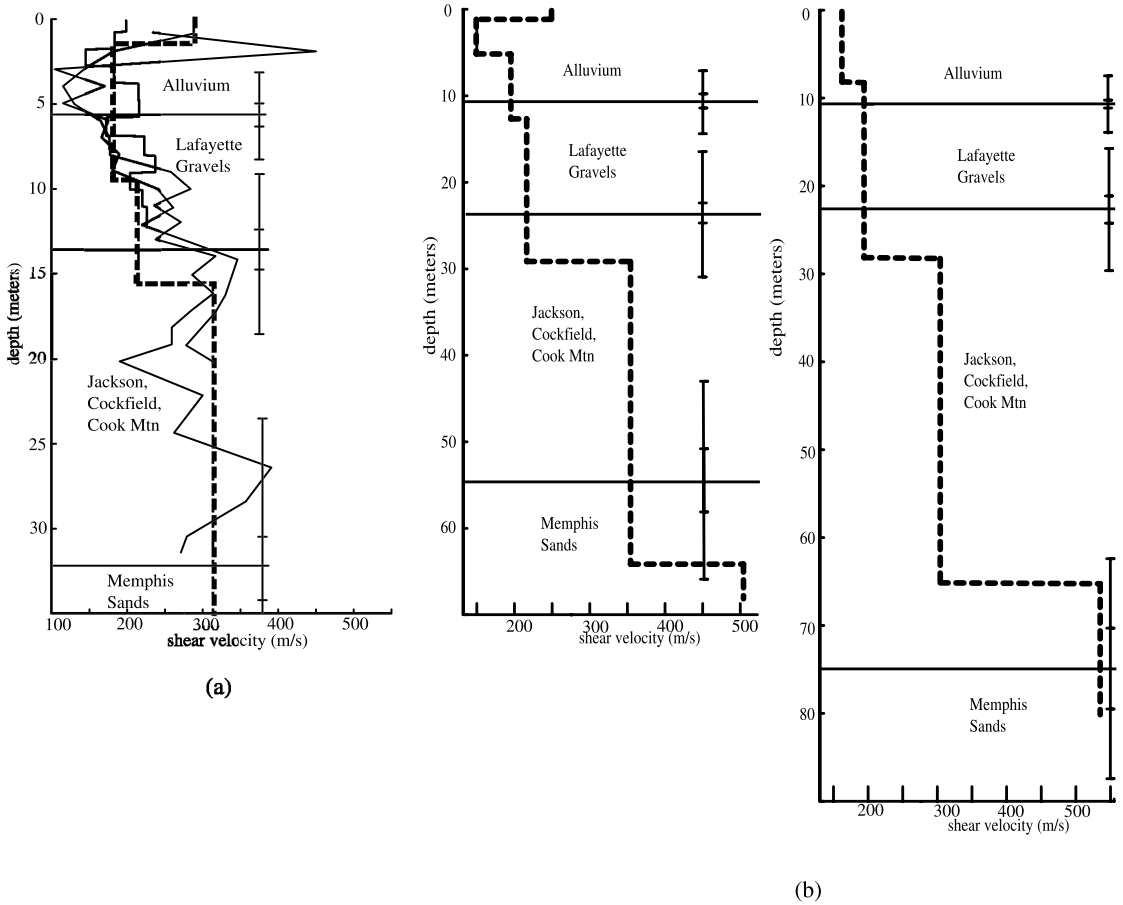


Figure 4. (a) Example shear-wave velocity profiles at a site where multiple profiles were measured (sites W12, M2, M3, and M4 along the Wolf River). The solid lines are interval measurements made with a piezocone (Schneider *et al.*, 2001), and the dashed line represents refraction measurement interpretation (Williams *et al.*, 2003). Depths and uncertainties to stratigraphic boundaries are estimated from the log data (vertical bars on right). The correspondence between the log and velocity interface depths is not clear in this case. (b) Two velocity profiles measured using refraction for sites near the Mississippi floodplain (left, W13; right, S4) with layer interface depths that agree with lithologic boundary depths within their uncertainties. Note the change in vertical scales between (a) and (b).

wave velocity characteristics needed for seismic hazard calculations. This suggests that our results should provide useful inputs to hazard calculations for Memphis.

Steidl (2000) studied southern California and defined site classes based on the surficial geology inferred from a 1:750,000-scale geologic map. He also examined the correlation between $V_s30$ and site amplification estimated from ground-motion recordings and between site class and site amplification. He found good correlation between $V_s30$ and site amplification, but the relationship between site class and site amplification was more variable and thus the correlation poorer. He speculated that the latter was because the surficial geology might not be adequately mapped at this scale and alone may not represent conditions at depth. In addition, poorer correlation between site class and amplification may reflect errors in measuring the amplification as well as true variability associated with propagation path and source differences. Steidl (2000) also concluded that the use of shear-wave velocity and geologic data together should provide useful constraints on site response and that much larger datasets that include ground-motion recordings are required to better understand and quantify the relationships between them all. Again, this suggests that our results should be useful in quantifying the hazard in Memphis. Although much less earthquake ground-motion data is available for the Memphis area than for California, the Williams *et al.* (2003) study documented differences in them that appeared to correlate with differences in near-surface shear-wave velocity.

We can now evaluate our initial assumption, that lithology correlates with shear-wave velocity. Although there is considerable overlap among the range of velocities estimated for each unit (Fig. 5; Table 1), the ranges are not so

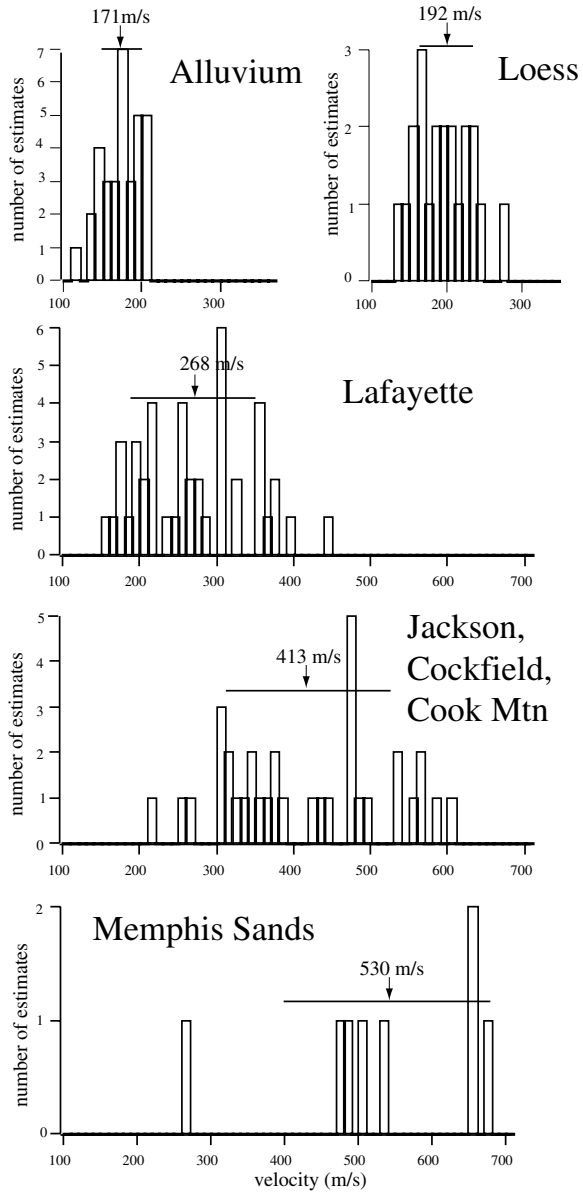


Figure 5. Histograms of shear-wave velocities associated with each lithologic layer for profiles shown at the locations in Figure 1. Velocities listed above each arrow are mean values, with horizontal lines beneath showing standard deviations. Median values differ insignificantly from the means (see Table 1). Note that we do not distinguish between Mississippi River alluvium and that along the other major waterways. Williams *et al.* (2003) found an average of 206 m/sec when only sites along the Mississippi were considered.

large that assignment of distinct velocities to each unit is reasonable, at least in the top ~30 m. These velocities are all quite low, such that significant ground-motion amplification and perhaps even ground failure may be significant in Memphis. Although the amount of data available for Memphis is very small relative to that for urban areas of California, we suggest that it may be equally useful given the relative simplicity of the geology in Memphis. The next step must be to use these results to derive estimates of the amplification. Albeit very small at present, the number of ground-motion recordings from Memphis and its vicinity is growing and must be employed to validate these estimates. Finally, this work has generated several products, including a three-dimensional model of the shallow subsurface geology beneath Memphis and a database of well log and boring log data useful for a wide variety of purposes.

## Acknowledgments

The authors thank Mark Petersen, Chuck Mueller, and two anonymous reviewers for their helpful reviews. This is CERI Contribution No. 444.

## References

Bodin, P., and S. Horton (1999). Broadband microtremor observation of basin resonance in the Mississippi embayment, Central U.S., *Geophys. Res. Lett.* **26,** 903–906.

Bodin, P., K. Smith, S. Horton, and H. Hwang (2001). Microtremor observations of deep sediment resonance in metropolitan Memphis, Tennessee, *Eng. Geol.* **62,** 159–169.

Broughton, A. T., R. B. VanArsdale, and J. H. Broughton (2001). Liquefaction susceptibility mapping in the city of Memphis and Shelby County, Tennessee, *Eng. Geol.* **62,** 207–222.

Cox, R. T., and R. B. VanArsdale (2002). The Mississippi embayment, North America: a first order continental structure generated by the Cretaceous superplume event, *J. Geodynam.* **34,** 163–176.

Dart, R. L., and H. S. Swolfs (1998). Contour mapping of relic structures in the Precambrian basement of the Reelfoot rift, North American midcontinent, *Tectonics* **17,** 235–249.

Field, E. H., and the SCEC Phase III Working Group (2000). Accounting for site effects in probabilistic seismic hazard analyses of southern California: overview of the SCEC Phase III Report, *Bull. Seism. Soc. Am.* **90,** S1–S31.

Fisk, H. N. (1939). Jackson Eocene from borings at Greenville, Mississippi, *Bull. Am. Assoc. Petrol. Geol.* **23,** 10.

Frankel, A., C. Mueller, T. Barnhard, D. Perkins, E. V. Leyendecker, N. Dickman, S. Hanson, and M. Hopper (1996). National seismic hazard maps: documentation, *U.S. Geol. Surv. Open-File Rept. 96-532*.

Frankel, A., C. Mueller, T. Barnhard, D. Perkins, E. V. Leyendecker, N. Dickman, S. Hanson, and M. Hopper (1997). Seismic hazard maps for the conterminous United States, *U.S. Geol. Surv. Open-File Rept. 97-131*, scale 1:7,000,000.

Graham, D. D., and W. S. Parks (1986). Potential for leakage among principal aquifers in the Memphis area, *U.S. Geol. Surv. Water Resources Invest. Rept. 85-4295*, 46 pp.

Johnston, A. C., and E. S. Schweig (1996). The enigma of the New Madrid earthquakes of 1811–1812, *Ann. Rev. Earth Planet Sci.* **24,** 339–384.

Kingsbury, J. A., and W. S. Parks (1993). Hydrogeology of the principal aquifers and relation of faults to interaquifer leakage in the Memphis area, TN, *U.S. Geol. Surv. Water Resources Invest. Rept. 93-4075*, 18 pp.

Lancaster, P., and K. Salkauskas (1986). Chap. 2 of *Curve and surface fitting: An Introduction*, Academic Press, London.

Mihills, R. K., and R. B. VanArsdale (1999). Late Wisconsin to Holocene New Madrid seismic zone deformation, *Bull. Seism. Soc. Am.* **89,** 1019–1024.

National Earthquake Hazards Reduction Program (NEHRP) (1997). Recommended Provisions for the Development of Seismic Regulations for New Buildings. I. Provisions. Prepared by the Building Seismic

Safety Council for the Federal Emergency Management Agency, Washington, D.C.

Parks, W. S., and J. K. Carmichael (1990). Geology and Ground-Water Resources of the Memphis Sand in Western Tennessee, *U.S. Geol. Surv. Water Resources Invest. Rept. 88-4182*, 30 pp.

Press, W. H., B. P. Flannery, S. A. Teukolsky, and W. T. Vetterling (1986). *Numerical Recipes: The Art of Scientific Computing*, Cambridge University Press, Cambridge.

Romero, S., and G. J. Rix (2001). Regional variations in near surface shear wave velocity in the greater Memphis area, *Eng. Geol.* **62,** 137–158.

Schneider, J. A., P. W. Mayne, and G. J. Rix (2001). Geotechnical site characterization in the greater Memphis area using cone penetration tests, *Eng. Geol.* **62,** 169–184.

Steidl, J. H. (2000). Site response in southern California for probabilistic seismic hazard analysis, *Bull. Seism. Soc. Am.* **90,** S149–S169.

Street, R., E. W. Woolery, Z. Wang, and J. B. Harris (2001). NEHRP soil classifications for estimating site-dependent seismic coefficients in the Upper Mississippi embayment, *Eng. Geol.* **62,** 123–136.

VanArsdale, R. B., and R. K. TenBrink (2000). Late Cretaceous and Cenozoic geology of the New Madrid seismic zone, *Bull. Seism. Soc. Am.* **90,** 345–356.

Williams, R. A., S. Wood, W. J. Stephenson, J. K. Odum, M. E. Meremonte, and R. Street (2003). Surface seismic refraction/reflection measurement determinations of potential site resonances and the areal uniformity of NEHRP site class D in Memphis, Tennessee, *Earthquake Spectra* **19,** 159–189.

Wills, C. J., M. Petersen, W. A. Bryant, M. Reichle, G. J. Saucedo, S. Tan, G. Taylor, and J. Treiman (2000). A site-conditions map for California based on geology and shear-wave velocity, *Bull. Seism. Soc. Am.* **90,** S187–S208.

## Appendix

In a standard least-squares problem we solve the set of equations

$$\begin{aligned} d_{\text{obs}}(x_1,y_1) &= b_1 + b_2\, x_1 + b_3\, y_1 + b_4\, x_1^2 \\ &\quad + b_5\, y_1^2 + b_6\, x_1\, y_1 \\ d_{\text{obs}}(x_N,y_N) &= b_1 + b_2\, x_N + b_3\, y_N + b_4\, x_N^2 \\ &\quad + b_5\, y_N^2 + b_6\, x_N\, y_N, \end{aligned} \tag{A1}$$

in which $d_{\text{obs}}(x_j,y_j)$, $j = 1, N$, are our $N$ observations at known locations $x_j,y_j$, $j = 1,N$, and $b_i$, $i = 1, 6$, are the unknowns we seek to find. Because $N > 6$ this is a standard overdetermined least-squares problem.

A standard least-squares solution to equation (A1) does not account for our belief that our polynomial model (equation A1) does not have enough degrees of freedom to represent the variability over the entire study area. To allow for greater variability laterally we allow the model to be a function of the location of interest at $x,y$, or equivalently the coefficients in equation (A1) become location dependent [*i.e.*, $b_i(x,y)$, $i = 1,6$]. We also apply a distance weighting to the observations before solving for $b_i(x,y)$, $i = 1,6$.

The implementation of this is more easily described by rewriting equation (A1) in matrix form:

$$\begin{vmatrix} d_{\text{obs}}(x_1,y_1) \\ \cdot \\ \cdot \\ \cdot \\ \cdot \\ \cdot \\ d_{\text{obs}}(x_N,y_N) \end{vmatrix} = \begin{vmatrix} 1 & x_1 & y_1 & x_1^2 & y_1^2 & x_1\, y_1 \\ \cdot & \cdot & \cdot & \cdot & \cdot & \cdot \\ \cdot & \cdot & \cdot & \cdot & \cdot & \cdot \\ \cdot & \cdot & \cdot & \cdot & \cdot & \cdot \\ \cdot & \cdot & \cdot & \cdot & \cdot & \cdot \\ \cdot & \cdot & \cdot & \cdot & \cdot & \cdot \\ 1 & x_N & y_N & x_N^2 & y_N^2 & x_N\, y_N \end{vmatrix} \begin{vmatrix} b_1(x,y) \\ \cdot \\ \cdot \\ \cdot \\ b_6(x,y) \end{vmatrix}$$

or

$$\mathbf{d}_{\text{obs}} = \mathbf{G}\ \mathbf{b}(x,y). \tag{A2}$$

We weight the observations, multiplying each by a factor that decreases with distance from $x,y$ to observation point $x_i,y_i$. Weights are described by the function

$$W(x,y,x_i,y_i) = 1/\{\sqrt{(x - x_i)^2 + (y - y_i)^2} + \varepsilon\}. \tag{A3}$$

The constant $\varepsilon$ prevents $W$ from becoming singular when the estimation and observation points are the same, and within some distance less than $\varepsilon$ all data are nearly equally weighted. Now the weighted least-squares problem to solve becomes

$$\mathbf{W}(x,y)\mathbf{d}_{\text{obs}} = \mathbf{W}(x,y)\ \mathbf{G}\ \mathbf{b}(x,y). \tag{A4}$$

With $\mathbf{b}(x,y)$ in hand we can now estimate the boundary depth at location $x,y$ (derive a locally appropriate model of the boundary). Our modeled boundary is

$$\begin{aligned} d_{\text{mod}}(x,y) &= b_1(x,y) + b_2(x,y)\, x + b_3(x,y)\, y \\ &\quad + b_4(x,y)\, x^2 + b_5(x,y)\, y^2 + b_6(x,y)\, xy. \end{aligned} \tag{A5}$$

Note that the polynomial constants, or model coefficients, of equation (A1) now differ for each estimation point, and we must solve the least-squares problem described by equation (A4) for each point.

## Estimating Uncertainties on Our Modeled Lithologic Boundaries

Assuming $d_{\text{mod}}(x,y)$ (equation A5) represents the true surface, a measure of the random error in the observations is the root mean square (rms) deviation between values predicted by the model and observed values. The data or rms error equals

$$\begin{aligned} \sigma_{\text{dat}} = \sum_{i=1}^{N} \{ W(x,y,x_i,y_i)^2\, [d_{\text{obs}}(x_i,y_i) \\ - d_{\text{mod}}(x_i,y_i)]^2 \} / \sum_{i=1}^{N} W(x,y,x_i,y_i)^2. \end{aligned} \tag{A6}$$

We also suspect that our model of the lithologic boundary is not a perfect representation of the true boundary, particularly in regions where there are few or no observations. To estimate this modeling uncertainty we employ a bootstrap procedure. Essentially this provides a measure of how sensitive the model is to the distribution of data. A bootstrap procedure employs repeated random resampling of the original dataset to provide a measure of the sensitivity to sampling without making assumptions about the underlying statistical distribution of the data. We resample our set of $N$ data, estimate a boundary depth using the moving-least-squares algorithm, and repeat this $M$ times. We resample with replacement; that is, we chose $N$ data by randomly selecting data indices from 1 to $N$ and allowing indices to be repeated (*Press et al.*, 1986). From these $M$ estimates we obtain a mean,

$$d_{\text{mean}} = 1/M \sum_{m=1}^{M} d_m(x,y), \tag{A7}$$

and standard deviation, which we refer to as a modeling error,

$$\sigma_{\text{mod}} = 1/(M - 1) \sum [d_m(x,y) - d_{\text{mean}}]^2. \tag{A8}$$

U.S. Geological Survey
3876 Central Ave., Suite 2
Memphis, Tennessee 38152-3050
(J.G., E.S., R.S., C.C.)

Ground Water Institute
The University of Memphis
300 Engineering Admin. Bldg.
Memphis, Tennessee 38152-3170
(B.W.)

Center for Earthquake Research & Information
The University of Memphis
3876 Central Ave., Suite 1
Memphis, Tennessee 38152-3050
(H.H., K.T.)

U.S. Geological Survey
640 Grassmere Park Dr.
Nashville, Tennessee 37211
(A.W., M.B.)

Dept. of Earth Sciences
The University of Memphis
113 Johnson Hall
Memphis, Tennessee 38152
(R.V.)

U.S. Geological Survey
MS 966
Box 25046
Denver Federal Center
Denver, Colorado 80225
(R.U., J.O., W.S., R.W.)

47 Woodbriar Court
Nicholasville, Kentucky 40356
(R.S.)

School of Civil & Environmental Eng.
Georgia Institute of Technology
Atlanta, Georgia 30332-0355
(P.M.)

U.S. Geological Survey
7777 Walnut Grove Rd.
Memphis, Tennessee 38120
(S.H.)

Manuscript received 31 July 2002.